Accepted Manuscript

Microstructure evolution and improved corrosion resistance of electrodeposited NiCo-Al composite coatings with different Al contents

Fei Cai, Xijun Cai, Shihong Zhang, Chuanhai Jiang

PII: S0925-8388(17)34117-8

DOI: 10.1016/j.jallcom.2017.11.335

Reference: JALCOM 44028

To appear in: *Journal of Alloys and Compounds*

Received Date: 26 July 2017

Revised Date: 6 November 2017

Accepted Date: 28 November 2017

Please cite this article as: F. Cai, X. Cai, S. Zhang, C. Jiang, Microstructure evolution and improved corrosion resistance of electrodeposited NiCo-Al composite coatings with different Al contents, *Journal of Alloys and Compounds* (2017), doi: 10.1016/j.jallcom.2017.11.335.

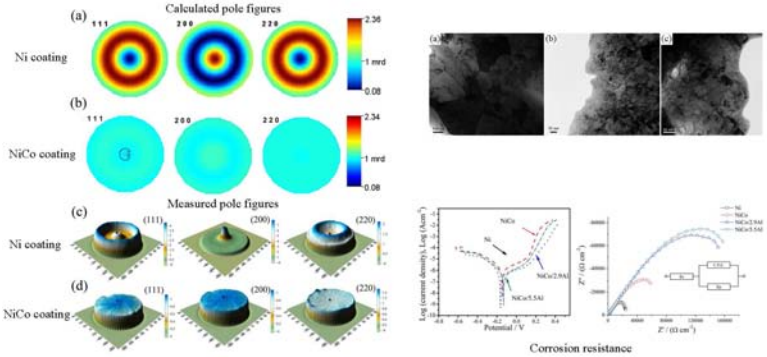

Microstructure evolution and improved corrosion resistance of electrodeposited NiCo-Al composite coatings with different Al contents

Fei Cai[a,*], Xijun Cai[a,b], Shihong Zhang[a,b*], Chuanhai Jiang[c]

[a]Research Center of Modern Surface and Interface Engineering, Anhui University of Technology, Maanshan City, Anhui Province 243002, PR China

[b]School of Materials Science and Engineering, Anhui University of Technology, Maanshan City, Anhui Province 243002, PR China

[c]School of Materials Science and Engineering, Shanghai Jiao Tong University, 800 Dongchuan Road, Shanghai 200240, PR China

Abstract:

In current work, pure Ni, NiCo, ***NiCo/2.9Al and NiCo/5.5Al*** coatings were fabricated by using electrodepositing method. X-Ray Diffraction (XRD), Rietveld while pattern fitting (RWPF), transmission electron microscope (TEM), potentiodynamic polarization and electrochemical impedance spectroscopy (EIS) experiments in 3.5 wt% NaCl solutions were used to investigate the effects of Al metal particles on the structure evolution and corrosion resistance of the investigated four coatings. Both the RWPF and TEM results showed that alloying with Co significantly decreased the ***crystallite size***. Furthermore, ***crystallite size*** was further reduced with the addition of Al micr-oparticles and smaller ***XRD crystallite size*** of 17 nm was obtained for

* Corresponding author. Tel.:+86 0555 2100060; fax.: +86 0555 21000108
E-mail address: caifei20150126@163.com (F. Cai)

NiCo/5.5Al composite coating. Measured pole figure and fitted pole figure exhibited the fiber texture for all the investigated coatings and addition of Co and Al suppressed the (200) texture of pure Ni coating and promoted the random orientation for the NiCo and NiCo-Al composite coating. Corrosion experiment results showed that, compared with Ni and NiCo coatings, addition of Al micro-particle could significantly increase the corrosion resistance. The ***NiCo/5.5Al*** composite coating exhibited the smaller corrosion current density of 0.581 $\mu A/cm^2$.

Keywords: Composite coating; Rietveld while pattern fitting; Texture; Corrosion resistance

1. Introduction

Protective hard chromium coatings often showed attractive properties such as corrosion resistance, hardness and wear resistance. However, environmental problems for the using toxic hexavalent chromium ions blocked its widespread use [1]. NiCo alloy coatings fabricated by electrodepositing usually exhibited higher hardness [2-6] and improved wear resistance [3, 5], which could be an ideal candidate for replacing hard chromium coatings. The main challenge for NiCo alloy might be the corrosion attack due to the low corrosion potential of Co compared with Ni.

The corrosion of the coatings could be minimized by addition of the second phase particles including TiO_2 [4], SiC [5, 7, 8] and Al_2O_3 [9-11] into the NiCo metal matrix. The main role of these particles in the coatings was to optimize microstructures of the NiCo based composite coatings or decrease contact area between the coating surface and corrosive medium. Shi et al. [5] confirmed the

enhancement in corrosion resistance and wear resistance of NiCo-SiC composite coatings with the addition of SiC particles. Other research also reported similar phenomenons in TiO_2 and Al_2O_3 particles [4, 9]. In addition, particle size also played an important role in microstructure and corrosion of the coating [7]. For example in NiCo-SiC composite coating, compared with micro-particles, SiC particle in nano-scale exhibited better corrosion resistance and higher hardness.

Due to their remarkable formation ability of passivation film, metal particles such as Al Cr and Zr have been successfully added into the Ni to enhance the corrosion [12-14]. These researches reported that continuous passive film formed on the surface could reduce further corrosion of the inner layer. Furthermore, texture change from (200) to (111) plane and decrease of grain size also resulted in the increase of anti-corrosion. Although the preparation and characterization of particles reinforced Ni and NiCo based composite coatings have been widely reported, the microstructure evolution and corrosion resistance of Al micro-particles enhanced NiCo-Al composite coating were few reported. In this study, the aim was to comparatively investigate the effects of micro-scale Al metal particle on structure evolution and corrosion resistance of the NiCo-Al composite coatings.

2. Experimental details

The specimens used in this work was stainless steel (1×1 cm^2) after a series of pretreatments including of grounding by using different emery papers, degreasing in 10% HCl acid and washing in distilled water, respectively. Detail depositing parameters were listed in Table.1. ***The SEM image of as-received Al power used to add into the bath was presented in Fig.1 and the power***

showed an average diameter of 1 µm. According to EDS analysis, the two investigated NiCo-Al composite coatings could be referred as to ***NiCo/2.9*** wt %Al and ***NiCo/5.5 wt% Al*** composite coating.

A JSM-7600F scanning electron microscope (SEM) was used to examine coating morphologies. Coating phase structure was examined by using Rigaku Ultima IV X-ray diffractometer employing Cu Kα radiation and operating at 40 kV and 30 mA in standard 2θ-θ mode. XRD whole pattern fitting of the coatings were done using a Rietveld refinement software MAUD to obtain the microstructure and texture information [15]. The measured pole figures the composite coating was determined by a Rigaku SmartLab X-ray diffractometer employing Cu Kα radiation (40 kV and 30 mA) with four-circle goniometer.

Two typical corrosion methods, namely electrochemical impedance spectroscopy (EIS) and potentiodynamic polarization experiments by using an CHI660E electrochemical apparatus were used to examine coating corrosion resistance. The standard three-electrode method was adopted, where the Ag/AgCl electrode [+207 mV(SHE)] was used as the reference electrode, the sample working was used as electrode (WE), platinum sheet was used as auxiliary electrode (AE). NaCl solution in the concentration of 3.5 wt % was adopted as the corrosion medium. The measurement temperature and scan rate wwer 25 ^{o}C and 1mV/s, respectively. To attain the steady state, each sample was immersed for about 40 min before the experiment. Tafel curves were used to determine corrosion potential (E_{corr}) and corrosion current density (I_{corr}). Concerning the EIS experiment, sinuous potential amplitude of 5 mV was applied and 0.01Hz to 100000 Hz of frequency range was used.

3. Results and Discussion

3.1 Surface morphology

To clarity the difference in surface morphologies for the investigated ***NiCo/Al*** coatings, the surface SEM experiment were conduced and the results are displayed in Fig. 2. ***For electrodeposited coatings, the typical pyramidal structures or globular structure were the agglomerated clusters or grains, and the changes in surface morphology were correlated with the evolution of grain size [16, 17].*** In this work, surface morphology of pure Ni coating (Fig. 2a and 2e) is presented for comparison which showed some regular pyramidal structures, ***indicating the lager crystallite size***. For ***NiCo*** alloy coating, the smaller globular structure appeared due to the addition of Co (Fig. 2b and 2f), ***which indicated the smaller crystallite size***. With addition of Al particles in the baths, the Al micro-particles were also observed on the surface of the ***NiCo/2.9Al and NiCo/5.5Al*** coatings (Fig. 2c, 2d, 2g and 2h). Particle distribution and contents in the composite played an important role in determining the microstructures and properties, especially the corrosion. In this paper, typical Al dot-map patterns for the ***NiCo/5.5Al*** coating are shown in Fig. 3 and it could be found that the Al micro-particles distributed uniformly over the ***NiCo/Al*** composite coating surface, which was good for improvement in corrosion resistance.

3.2 Microstructure analysis

XRD patterns of the investigated coatings are presented in Fig. 4. Diffraction peaks of Ni or NiCo (111), (200), (220), (311) and (222) planes were detected for all the coatings. Addition of 44 wt % Co decreased the diffraction peak intensities and broadened the NiCo diffraction peaks. However, no evident changes in the ***NiCo/Al*** coating XRD patterns witht further incorporation of Al micro-particles in the coatings.

In addition, Al peak was also detected as shown in ***NiCo/5.5Al*** composite coating (as inserted in Fig. 4).

Fig.5 (a) and (b) show the typical Rietveld XRD refinement pattern of pure Ni and NiCo coating. The final R_w (%) and Sigma values, meaning the goodness of fitting, for all the refinements of XRD patterns are below 2.0 and 2.0, respectively. By using Rietveld method, ***it could be found that the crystallite size*** decreased and distributed more uniformly in the order of Ni, NiCo, ***NiCo/2.9Al and NiCo/5.5Al coating*** (Fig.5c). And crystallite size the as-deposited coatings was calculated and also shown in Table.2. For pure Ni coating, the crystallite size of 152 nm was obtained. For NiCo alloy coating, the crystallite size sharply decreased to 25 nm. However, addition of 2.9 wt% Al particles slightly reduced the crystallite size to 19 nm, and further addition of 5.5 wt% Al particles decreased the crystallite size to 17 nm, indicating that grain refining effect could be caused by addition of Al particles in this work. Similar grain refining caused by Co element and second particles were also reported [18, 19].

To further confirm the grain size change caused by addition of Co element and Al micro-particle, TEM experiments were conducted on pure Ni coating, NiCo alloy coating and ***NiCo/5.5 Al*** composite coating and the results are presented (Fig.6 and Fig. 7). The pure Ni coating showed the lager grain with clear interface (Fig.6a), while alloying with Co element resulted in the sharp decrease in ***crystallite size*** (Fig.6b). TEM and HR-TEM image of NiCo-5.5Al composite coating were presented in Fig. 7. Diffuse microstructure was found for the ***NiCo/5.5Al*** composite coating and

similar results also were reported in NiCo and NiCu coating [18]. The HR-TEM (Fig. 7b) showed the typical characteristics of nano-crystalline. ***Based on the TEM analysis, the Ni, NiCo and NiCo/5.5Al coatings showed the average crystallite size of 320 nm, 35 nm and 25 nm, which were more than those determined from the XRD. The crystallite size of investigated coatings from XRD was not consistent with that measured by TEM due to their higher micro-strain induced by the stress of the coatings [20]. Both the TEM and XRD results showed that alloying with Co and addition of Al decreased the crystallite size of the coatings.***

3.2 Texture analysis

For coatings prepared by electrodepositing technology, texture was one of the typical characteristic. In this study, for the XRD patterns of pure Ni, the (200) peak intensity was more than other peaks, indicating the typical (200) preferred orientation for pure Ni coating obtained from the Watts solution. However, addition of 44 wt. % Co promoted the growth of the (111) and (220) planes, depressed the growth of the (200) plane. In this work, Maud software was used to fit the texture of the electrodeposited coatings. Typical fiber texture for pure Ni coating and ***NiCo*** alloy coating were found, and the investigated coatings exhibited the (200) texture and random orientation (Fig.8a and 8b), respectively. Furthermore, the measured pole figures are also presented to confirm the calculated pole figures (Fig.8c and 8d). From Fig.8c and Fig. 8d, the measured pole figure showed evolution from typical (200) fiber texture for the pure Ni depositing coating to the random orientation for ***NiCo*** alloy coating (shown in Fig. 8d). The measured pole figure results were in agreement

with the calculated pole figure, indicating that alloying of Co could restrain the (200) texture of pure Ni coating.

3.4 Corrosion resistance

To examine corrosion performance of the investigated four coatings, potentiodynamic polarization and electrochemical impedance spectroscopy experiments were adopted. Potentiodynamic polarization curves for investigated coatings are depicted in Fig. 9 and corresponding corrosion potential (E_{corr}) and corrosion current density (I_{corr}) are summarized Table.3. Given the larger I_{corr} value of 7.206 μA/cm^2 for the pure Ni coating, I_{corr} of the NiCo alloy was 1.515 μA/cm^2, indicating significant increase in anti-corrosion. This corrosion resistance enhancement could be due to the formation of smoother surface [21]. Furthermore, addition of 2.9 wt% Al particles further reduced the I_{corr} to 0.635 μA/cm^2, which was more than twice as compared with the NiCo alloy coating. However, I_{corr} showed a slight decrease to 0.581 μA/cm^2 with further addition of 5.5 wt% Al particles. The improvement in corrosion resistance might be due to the addition of Al particle, which could form the protective Al_2O_3 passive film on the coating surface and suppress the further corrosion of the inner layer [22]. Similar phenomenon about the improvement in corrosion resistance by addition of metal particles such as Al and Zr were also reported [12, 22]. In addition, the grain size also played an important role in corrosion resistance. Some research reported that smaller grain size increased the path of corrosion medium from the surface to substrate.

To get more information about the corrosion behavior of the coating, EIS experiment was conducted and the results are ploted in Fig.10. It could be found from

Fig. 10 that all the as-deposited composite coatings showed a single semicircle, meaning the diffusely controlled corrosion process. And the single semicircle also indicated only one time constant for which electrochemical process occurred at the interface between electrodes and electrode. The equivalent circuit (as inserted in Fig.10) was proposed to fit the impedance spectra and the extracted results from the EIS by simulation are listed in Table.4. The solution resistance *Rs* showed no obvious change. The *Rp* value, referred to the corrosion resistance, showed an increase in the order of Ni, NiCo, ***NiCo/2.9Al and NiCo/5.5Al***, indicated the increasing corrosion resistance. The obtained EIS results agreed well with the potentiodynamic polarization that addition of Al micro-particle improved the corrosion resistance of the investigated coatings.

4. Conclusions

In this work, pure Ni, NiCo, ***NiCo/2.9 Al and NiCo/5.5*** Al were fabricated by using electrodepositing method. Different methods were applied to investigate the effects of Al metal particles on the microstructure evolution and corrosion resistance. Compared with 152 nm for pure coating, alloying with Co significantly decreased the ***crystallite size*** to 25 nm and smaller ***crystallite size*** of 17 nm was obtained for ***NiCo/Al*** with addition of 5.5 wt% Al particles. Typical fiber texture characteristic was observed for all the electrodeposited coatings by using the measured and fitted pole figures. The (200) texture for pure Ni was significantly suppressed and random orientation was promoted for the NiCo based coatings, which might be due to alloying with Co element and adding of second Al micro-particles. Compared with Ni and NiCo

coatings, NiCo-Al composite coating exhibited significant improvement in corrosion resistance with addition of metal Al particles. The smaller corrosion current density of 0.581 μA/cm^2 was exhibited for the ***NiCo/5.5 Al*** composite coating.

Acknowledgements

This work was supported by the National Science Foundation of China (Grant no. 51671002) and the Anhui University of Technology 2016 Youth Fund (RD16100252).

References

[1] Liju Elias, A. Chitharanjan Hegde, Effect of magnetic field on corrosion protection efficacy of Ni-W alloy coatings, J. Alloys. Comp. 712 (2017) 618-626.

[2] Meenu Srivastava, V. Ezhil Selvi, V.K. William Grips, K.S. Rajam, Corrosion resistance and microstructure of electrodeposited nickel–cobalt alloy coatings, Surf. Coat. Technol. 201 (2006) 3051-3060.

[3] L. Shi, C.F. Sun, P. Gao, F. Zhou, W.M. Liu, Electrodeposition and characterization of Ni-Co-carbon nanotubes composite coatings, Surf. Coat. Technol. 200 (2006) 4870- 4875

[4] B. Ranjith, G. Paruthimal Kalaignan, Ni-Co-TiO_2 nanocomposite coating prepared by pulse and pulse reversal methods using acetate bath, Appl. Surf. Sci. 257 (2010) 42-47.

[5] Lei Shi, Chufeng Sun, Ping Gao, Feng Zhou, Weimin Liu, Mechanical properties and wear and corrosion resistance of electrodeposited Ni-Co/SiC nanocomposite coating, Appl. Surf. Sci. 252 (2006) 3591-3599.

[6] Meenu Srivastava, V.K. William Grips, K.S. Rajam, Electrodeposition of Ni-Co composites containing nano-CeO_2 and their structure, properties, Appl. Surf. Sci. (2010) 717-722.

[7] Babak Bakhit, Alireza Akbari, Effect of particle size and co-deposition technique on hardness and corrosion properties of Ni-Co/SiC composite coatings, Surf. Coat. Technol. 206 (2012)

4964-4975.

[8] Babak Bakhit, Alireza Akbari, Farzad Nasirpouri, Mir Ghasem Hosseini, Corrosion resistance of Ni-Co alloy and Ni–Co/SiC nanocompositecoatings electrodeposited by sediment codeposition technique, Appl. Surf. Sci. 307 (2014) 351-359.

[9] B.R. Tian, Y.F. Cheng, Electrolytic deposition of Ni-Co-Al_2O_3 composite coating on pipe steel for corrosion/erosion resistance in oil sand slurry, Electrochim. Acta. 53 (2007) 511-517.

[10] Geta Carac, Adriana Ispas, Effect of nano-Al_2O_3 particles and of the Co concentration on the corrosion behavior of electrodeposited Ni-Co alloys, J. Solid. State. Electrochem. (2012) 16:3457-3465.

[11] L.M. Chang, H.F. Guo, M.Z. An, Electrodeposition of Ni-Co/Al_2O_3 composite coating by pulse reverse method under ultrasonic condition, Mater. Lett 62 (2008) 3313-3315.

[12] Fei Cai, Chuanhai Jiang, Influences of Al particles on the microstructure and property of electrodeposited Ni-Al composite coatings, Appl. Surf. Sci. (2014) 620-625.

[13] ZHOU Yue-bo, ZHAO Guo-gang, ZHANG Hai-jun, Fabrication and wear properties of co-deposited Ni-Cr nanocomposite coatings, Trans. Nonferrous Met. Soc. China 20(2010) 104-109.

[14] Fei Cai, Chuanhai Jiang, Zhongquan Zhang, Enzo Muttini, Peng Fu, Yuantao Zhao, Vincent Ji, Fabrication and characterization of Ni-Zr composite coatings using electrodepositing technique, J. Alloys. Comp 635 (2015) 73-81.

[15] L. Lutterotti, Maud version 2.33, 2011. (http://www.ing.unitn.it/maud/).

[16] Zhongquan Zhang, Chuanhai Jiang, Fei Cai, Peng Fu, Naiheng Ma, Vincent. Two stages for the evolution of crystallite size and texture of electrodeposited Ni-ZrC composite

coating, Surf. Coat. Technol. 261 (2015) 122-129;

[17] P. Angerer, H. Simunkova, E. Schafler, M.B. Kerber, J. Wosik, G.E. Nauer, Structure and texture of electrochemically prepared nickel layers with co-deposited zirconia nanoparticles, Surf. Coat. Technol.. 203 (2009) 1438-1443.

[18] Ze Chai, Chuanhai Jiang, Yuantao Zhao, Chengxi Wang, Kaiyuan Zhu, Fei Cai, Microstructural characterization and corrosion behaviors of Ni-Cu-Co coatings electrodeposited in sulphate-citrate bath with additives, Surf. Coat. Technol. 307 (2016) 817-824.

[19] M.H. Sarafrazi, Morteza Alizadeh, Improved characteristics of Ni-electrodeposited coatings via the incorporation of Si and TiO_2 particulate reinforcements, J. Alloys. Comp. 720 (2017) 289-299.

[20] C. Ma, S. C. Wang, C. T. J. Low, L. P. Wang and F. C. Walsh, Effects of additives on microstructure and properties of electrodeposited nanocrystalline Ni-Co alloy coatings of high cobalt content, T. I.Met.Finish, 2014, 92 (4), 189-195.

[21] Xiaokui Yang, Qing Li, Shiyan Zhang, Hui Gao, Fei Luo, Yan Dai, Electrochemical corrosion behaviors and corrosion protection properties of Ni-Co alloy coating prepared on sintered NdFeB permanent magnet, J. Solid. State. Electrochem. (2010) 14:1601-1608.

[22] Fei Cai, Chuanhai Jiang, Xueyan Wu, X-ray diffraction characterization of electrodeposited Ni-Al composite coatings prepared at different current densities, J. Alloys. Comp. 604 (2014) 292-297.

Figure captions:

Fig. 1 SEM image of the as-received Al power

Fig. 2 Surface morphology images of (a, e) pure Ni, (b, f) ***NiCo*** (c, g) ***NiCo/2.9Al and NiCo/5.5Al*** (d, h) at two different magnifications: 1000× and 3000×

Fig. 3 The element dot-map of the ***NiCo/5.5Al*** composite coatings

Fig. 4 XRD patterns of pure Ni, ***NiCo***, ***NiCo/2.9Al and NiCo/5.5Al*** coatings

Fig. 5 Typical Rietveld while pattern fitting for (a) pure Ni coating, (b) NiCo coating and (c) distribution of crystallite size of the investigated four coatings.

Fig. 6 TEM images of pure (a) Ni coating and (b) ***NiCo*** alloy coatings

Fig. 7 TEM images of (a) ***NiCo/5.5Al*** coating and (b) corresponding HR-TEM

Fig. 8 Calculated pole figures of (a) pure Ni coating and (b) NiCo alloy coating and measured pole figures of (c) pure Ni coating and (d) NiCo alloy coating

Fig. 9 Potentiodynamic polarization curves for coatings in 3.5 % NaCl solution

Fig. 10 EIS curves for coatings in 3.5 % NaCl solution

Table captions:

Table. 1 Depositing parameters for investigated coatings

Table. 2 ***Crystallite size*** and microstrain obtained from the Rietveld while pattern fitting method

Table. 3 Corrosion potential E_{corr} and corrosion current I_{corr} of the coatings

Table. 4 Fitting of corrosion parameters from the measured EIS plots on composite coatings of the coatings

Table. 1

Coatings	Composition of nicke solution (g/L)						Operating conditions
	Nickel sulfate	Nickel chloride	Boric acid	cobaltous sulfate	Sodium dodecyl sulfate	Al particle (1 μm)	
Pure Ni	240	40	30	—	0.2	—	Temperature: 50 °C
NiCo	240	40	30	20	0.2	—	pH: 4.2
NiCo/2.9Al	240	40	30	20	0.2	50	Time: 1 hr
NiCo/5.5Al	240	40	30	20	0.2	100	Current density: 4 A/dm^2
							Stir rate: 300 rpm

Table. 2

Coatings	*Crystallite size* (nm)	*Microstrain*
Ni	152	5.98×10^{-4}
NiCo	25	12.9×10^{-4}
NiCo/2.9Al	19	13.1×10^{-4}
NiCo/5.5Al	17	13.4×10^{-4}

Table. 3

	E_{corr} (mV)	I_{corr} (μA/cm^2)
Ni	-174.1	7.206
NiCo	-144.7	1.515
NiCo/2.9Al	-163.2	0.635
NiCo/5.5Al	-132.3	0.581

Table. 4

As-deposited coatings	*Rs*(Ω cm^{-2})	*Rct*(kΩ cm^{-2})	*CPE*(μF cm^{-2})	*n*
Ni	8.6	25.2	70	0.90
NiCo	6.6	105.3	27.5	0.92
NiCo/2.9Al	5.8	174.2	24.4	0.89
NiCo/5.5Al	5.9	184.5	24.5	0.89

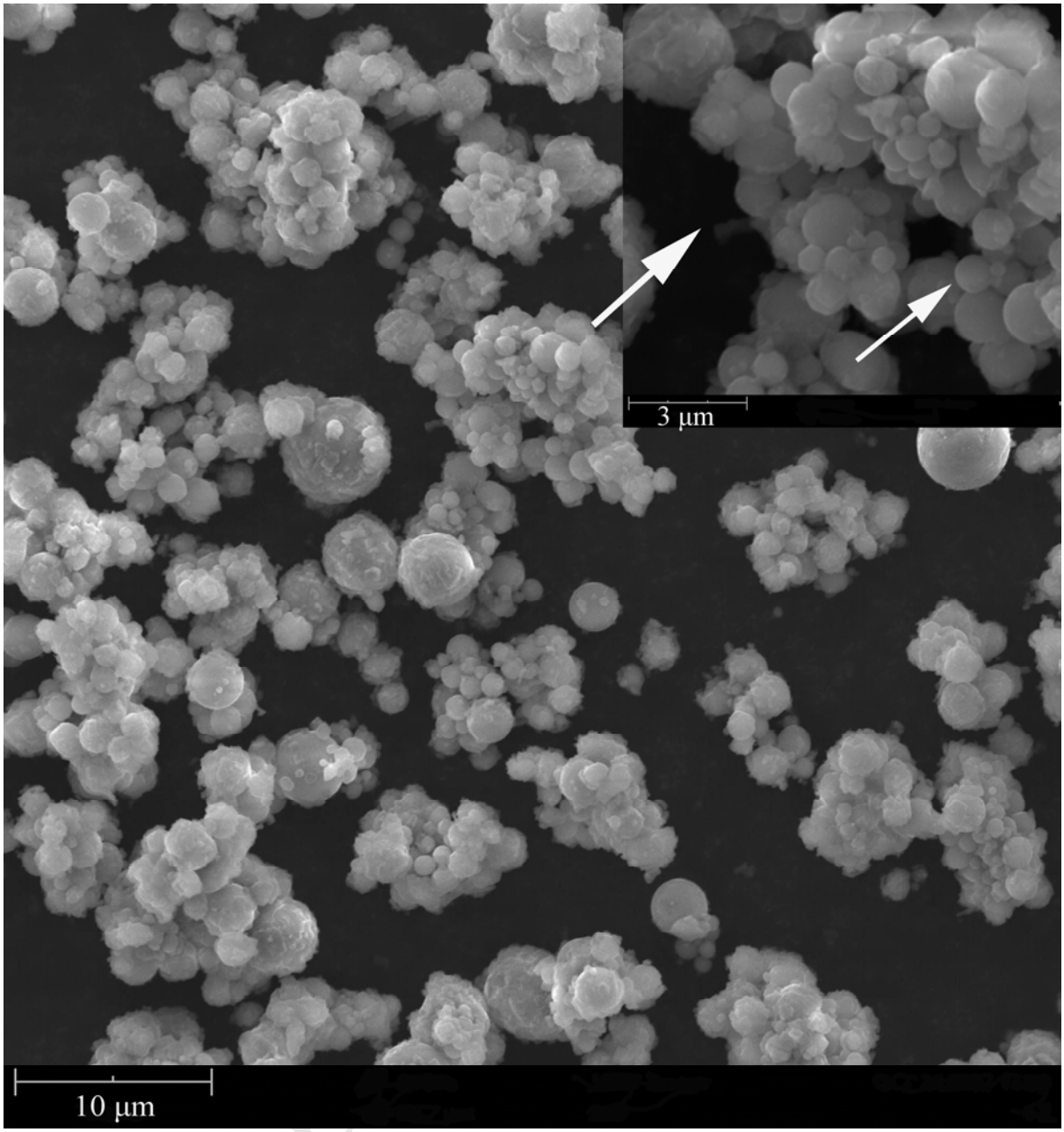

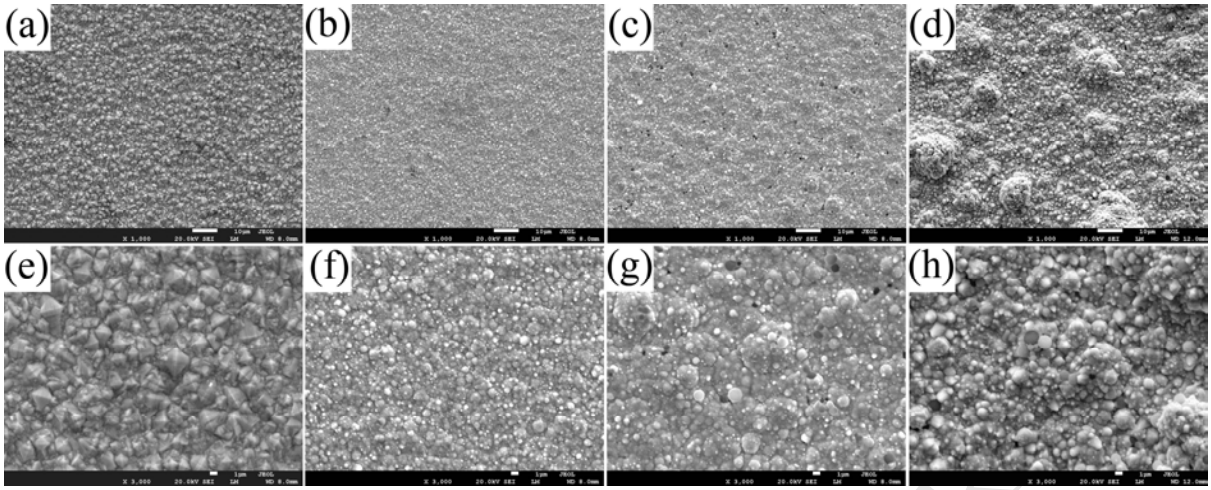

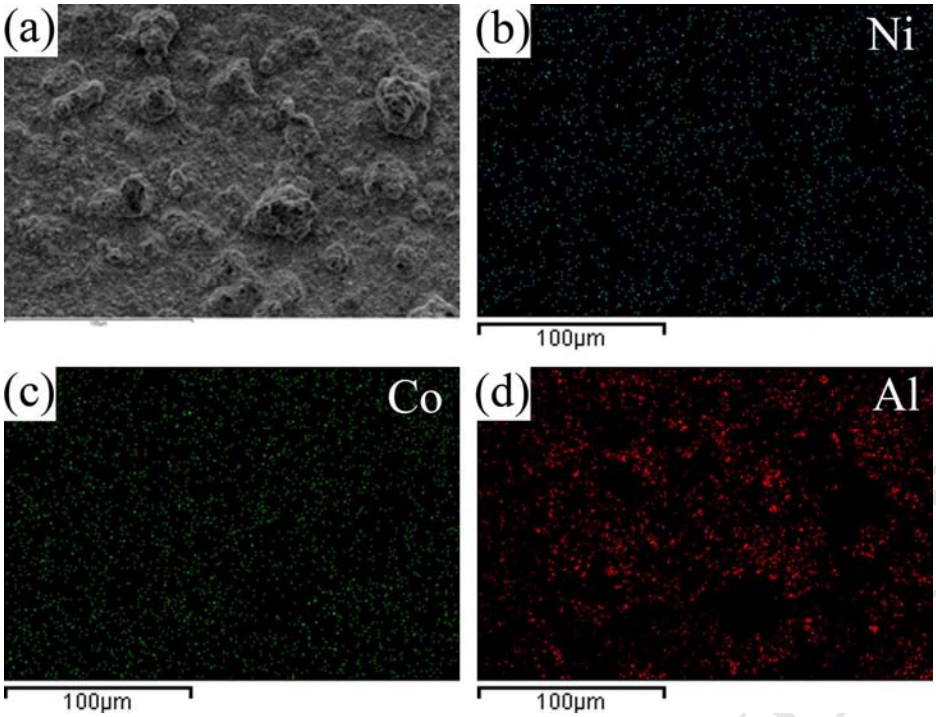

Fig.4

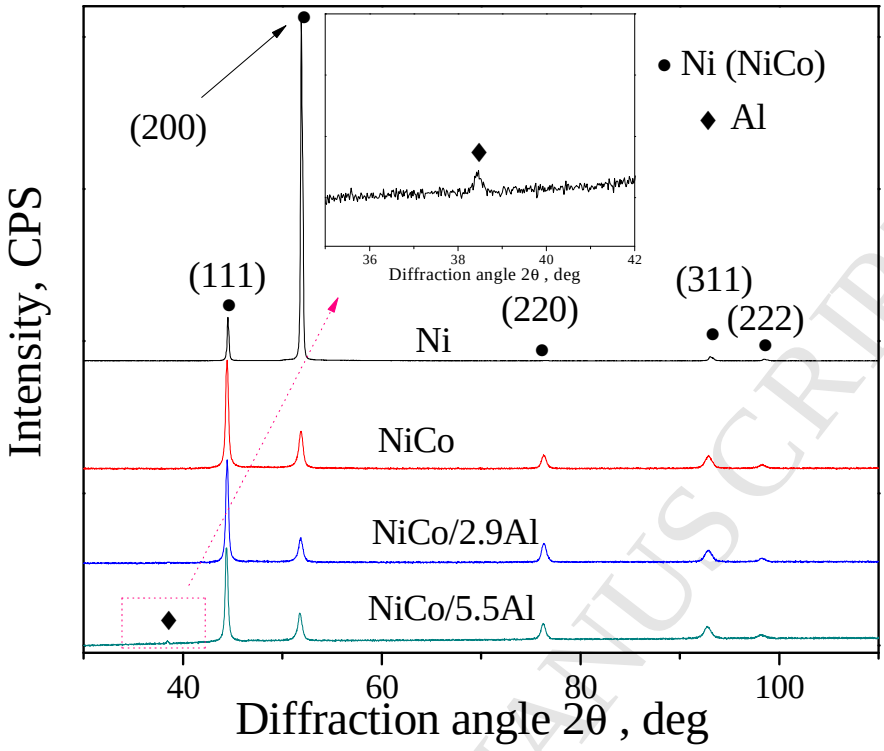

(a)

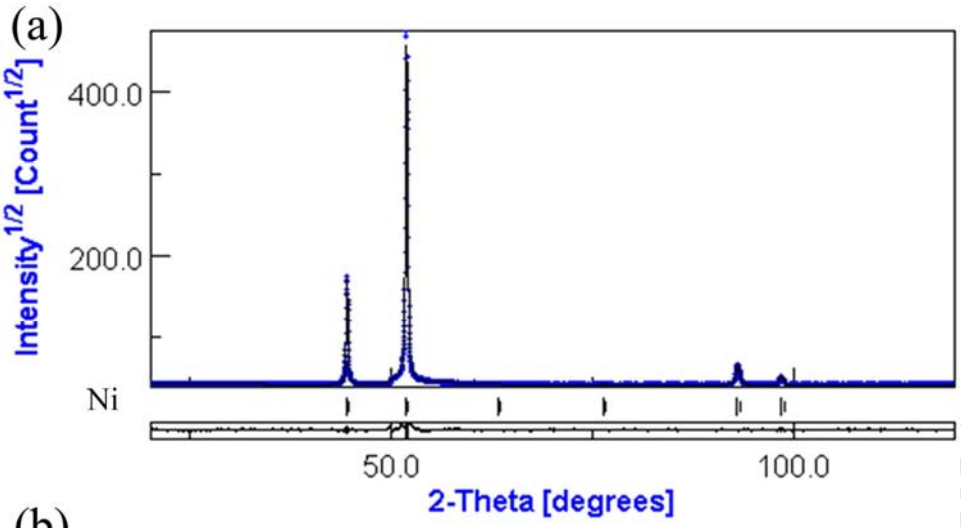
Intensity$^{1/2}$ [Count$^{1/2}$]
400.0
200.0
Ni
50.0
100.0
2-Theta [degrees]

(b)

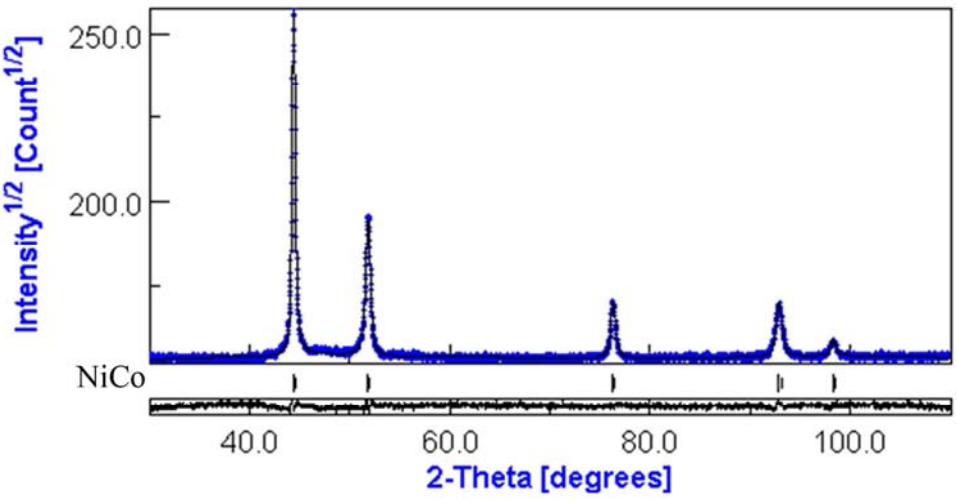
Intensity$^{1/2}$ [Count$^{1/2}$]
250.0
200.0
NiCo
40.0
60.0
80.0
100.0
2-Theta [degrees]

(c)

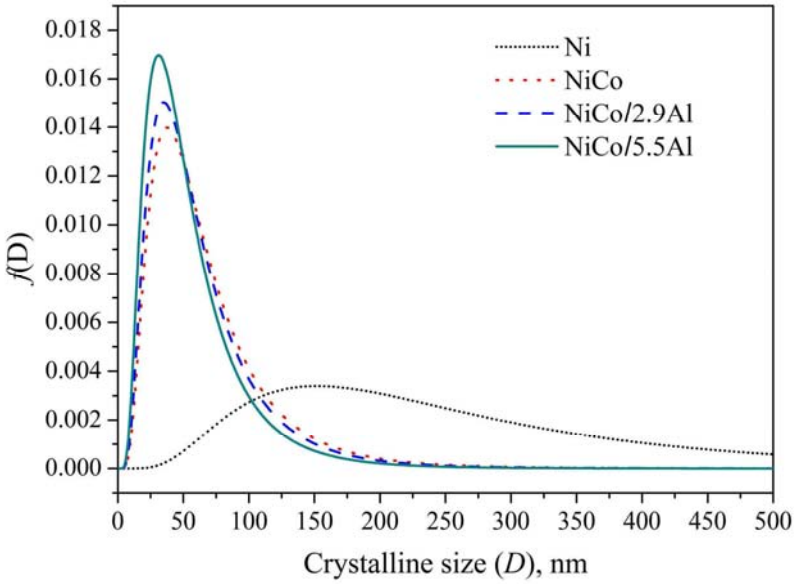
f(D)
0.018
0.016
0.014
0.012
0.010
0.008
0.006
0.004
0.002
0.000
0
50
100
150
200
250
300
350
400
450
500
Crystalline size (D), nm
Ni
NiCo
NiCo/2.9Al
NiCo/5.5Al

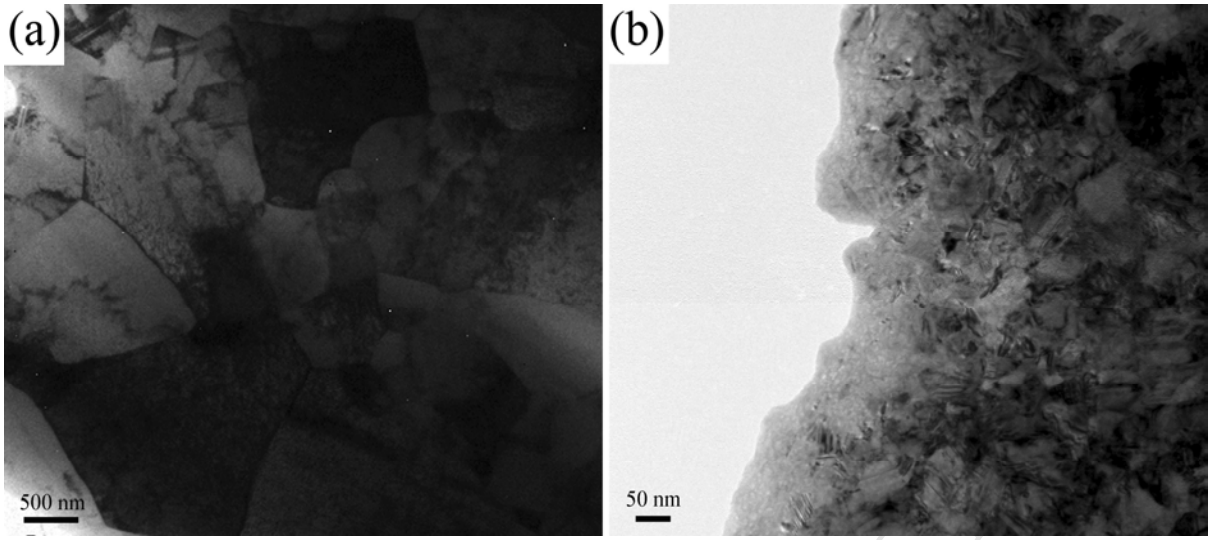

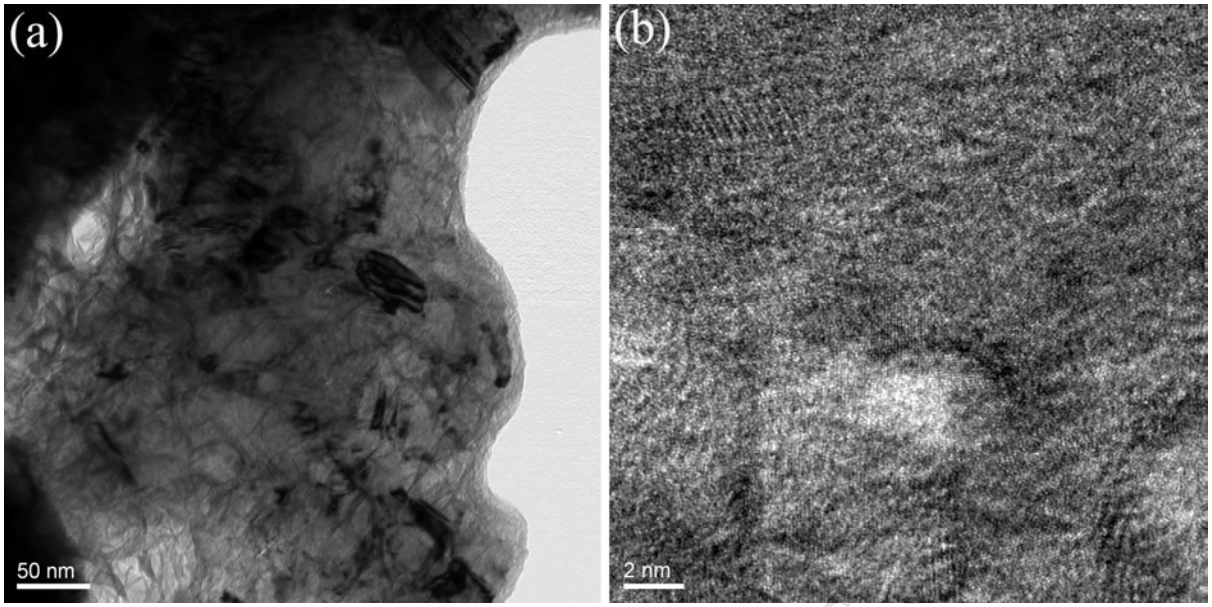

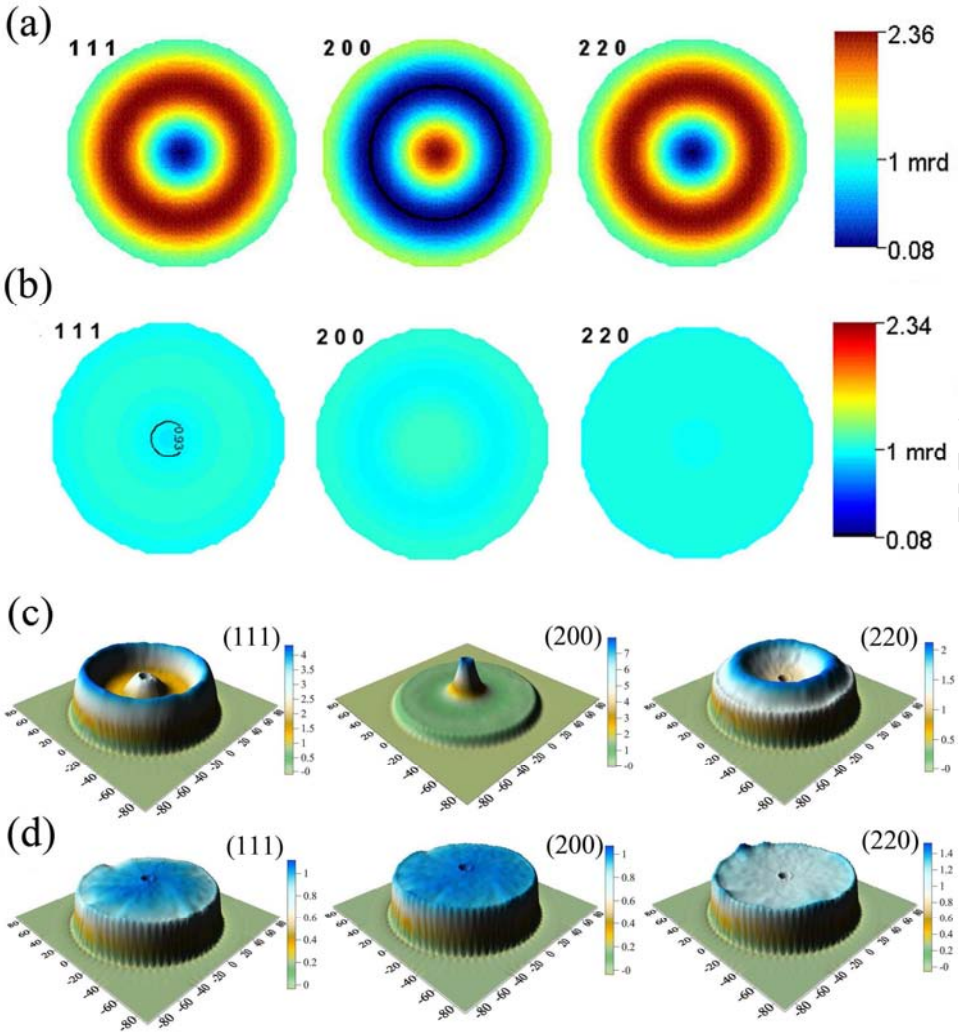

Fig.9

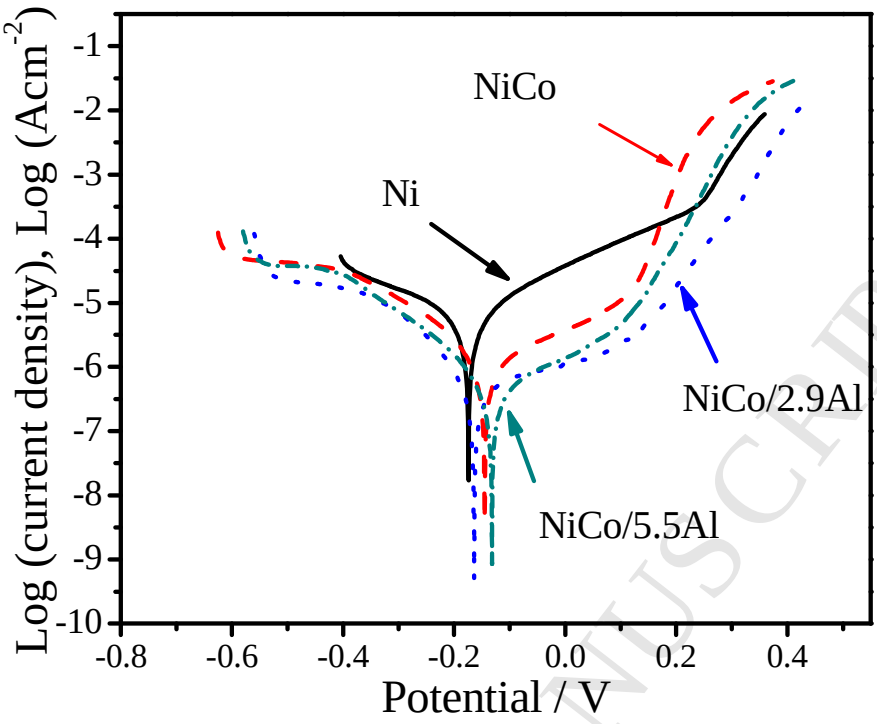

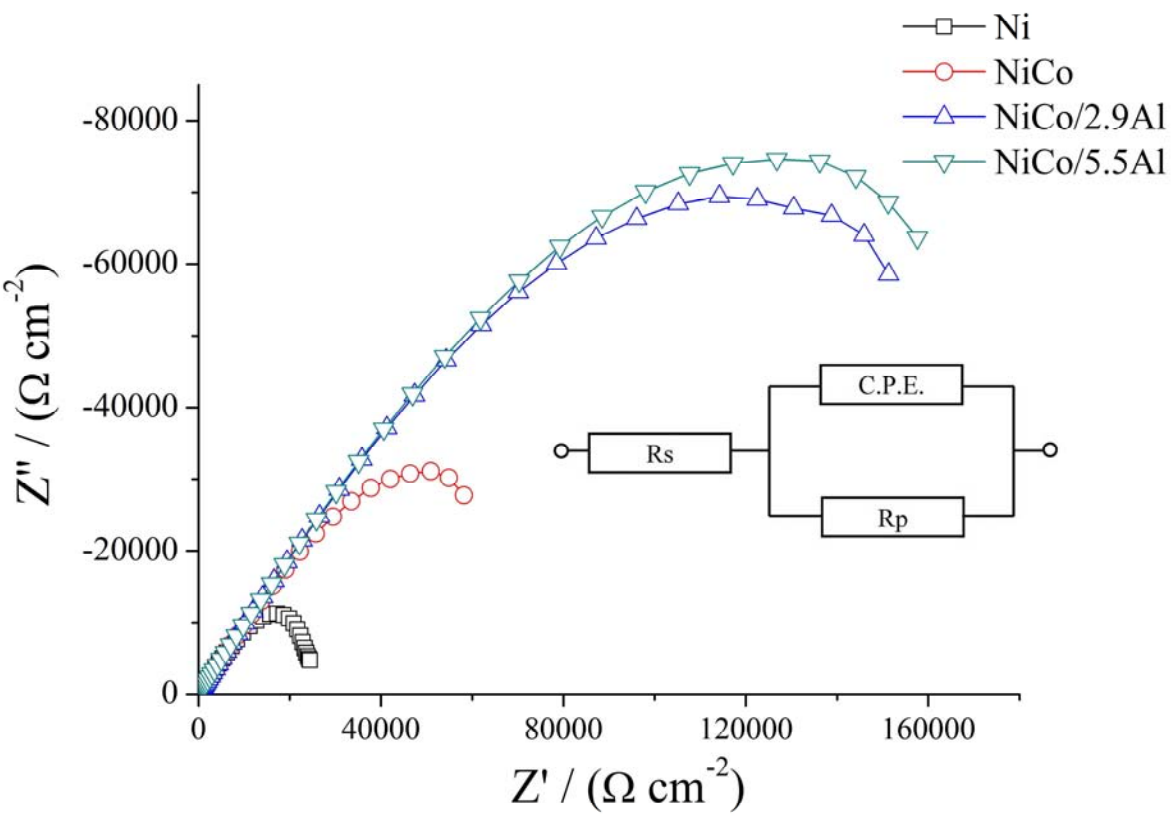

(1) NiCo/Al coatings with different Al contents were fabricated;

(2) Rietveld while pattern fitting method was used to determine the structures and texture;

(3) Effects of Al particles on microstructure and corrosion were investigated.